Supplement of Hydrol. Earth Syst. Sci., 26, 5721–5735, 2022
https://doi.org/10.5194/hess-26-5721-2022-supplement

Hydrology and Earth System Sciences
Open Access
EGU

Supplement of

Precipitation biases and snow physics limitations drive the uncertainties in macroscale modeled snow water equivalent

Eunsang Cho et al.

Correspondence to: Eunsang Cho (eunsang.cho@nasa.gov)

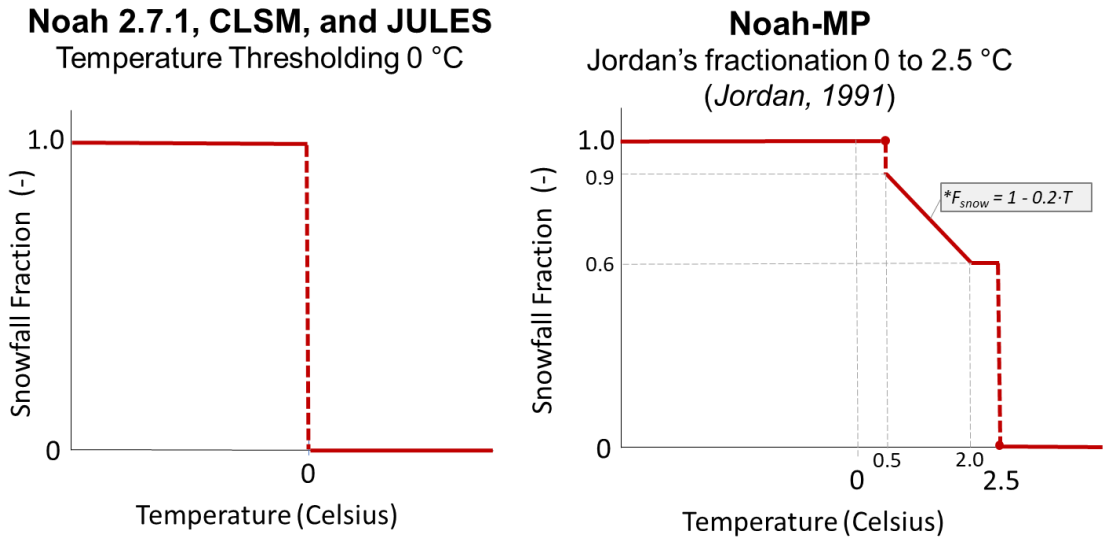

Figure S1. Schematic diagrams of the two precipitation partitioning methods, single threshold method (Catchment, JULES, and Noah) and Jordan's fractioning method (Noah-MP)

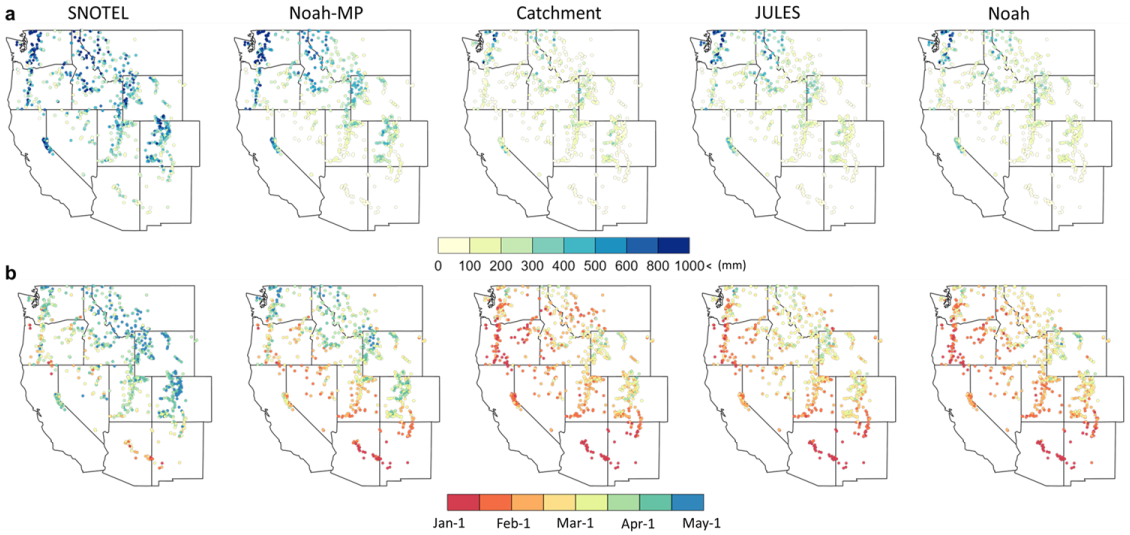

Figure S2. (a) Mean annual maximum SWE maps of SNOTEL observations and the four LSMs averaged over the three forcings and (b) mean date maps when the annual maximum SWE occurs from 2010 to 2017 across the western United States

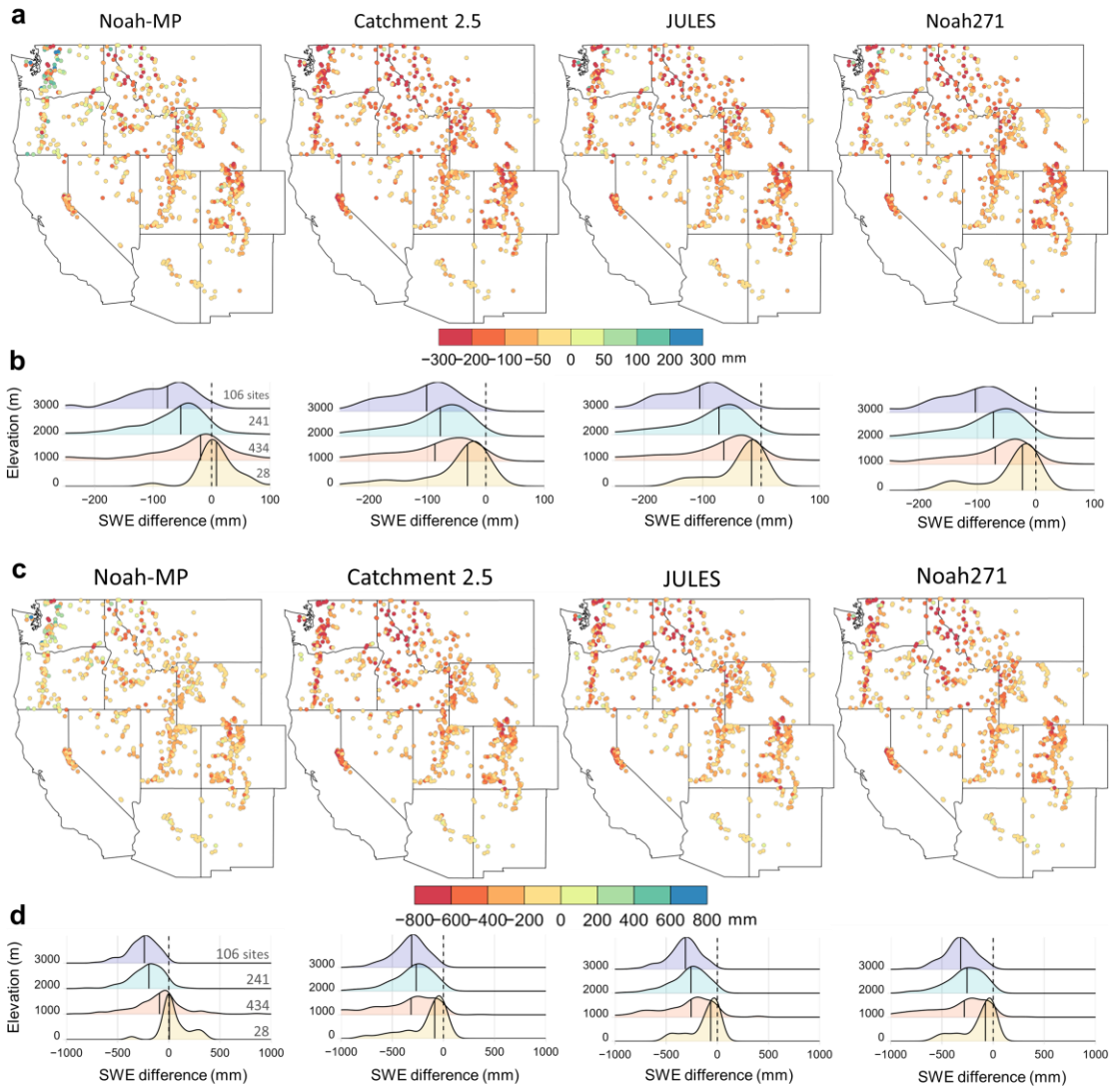

Figure S3. (a) Mean difference maps in annual mean SWE between four LSM estimates and SNOTEL (four LSMs ensembled by three forcings minus SNOTEL) from 2010 to 2017, (b) density plots of the annual mean SWE difference by four elevation ranges of SNOTEL sites. Similarly, (c) mean difference maps in the April 1st SWE from 2010 to 2017, and (d) density plots of the April 1st SWE difference by four elevation ranges of SNOTEL sites across the western United States

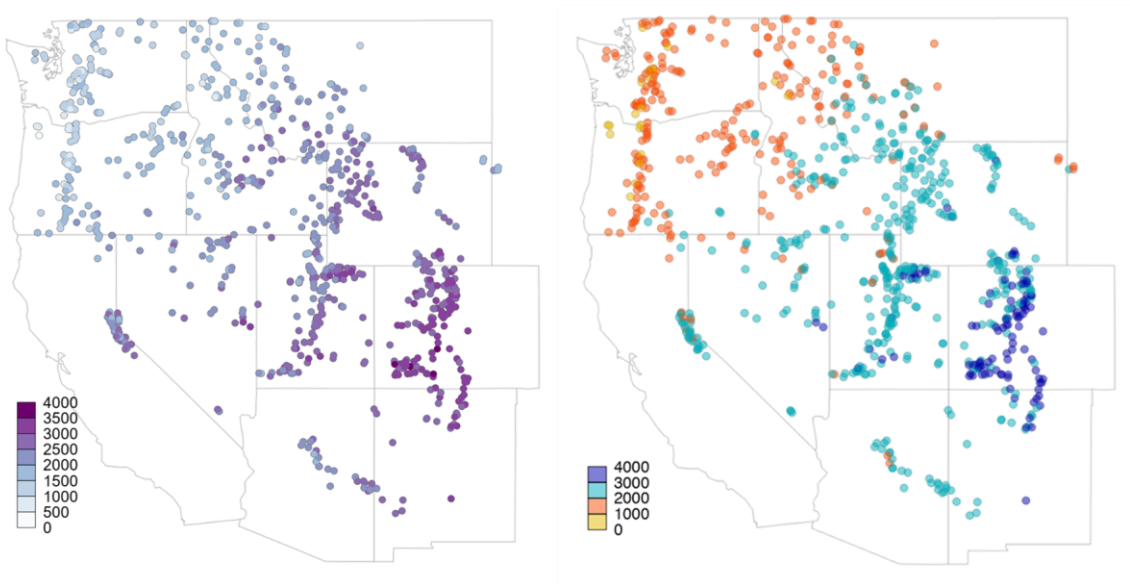

Figure S4. Elevation maps of SNOTEL sites across the western United States with continuous and four different elevation ranges

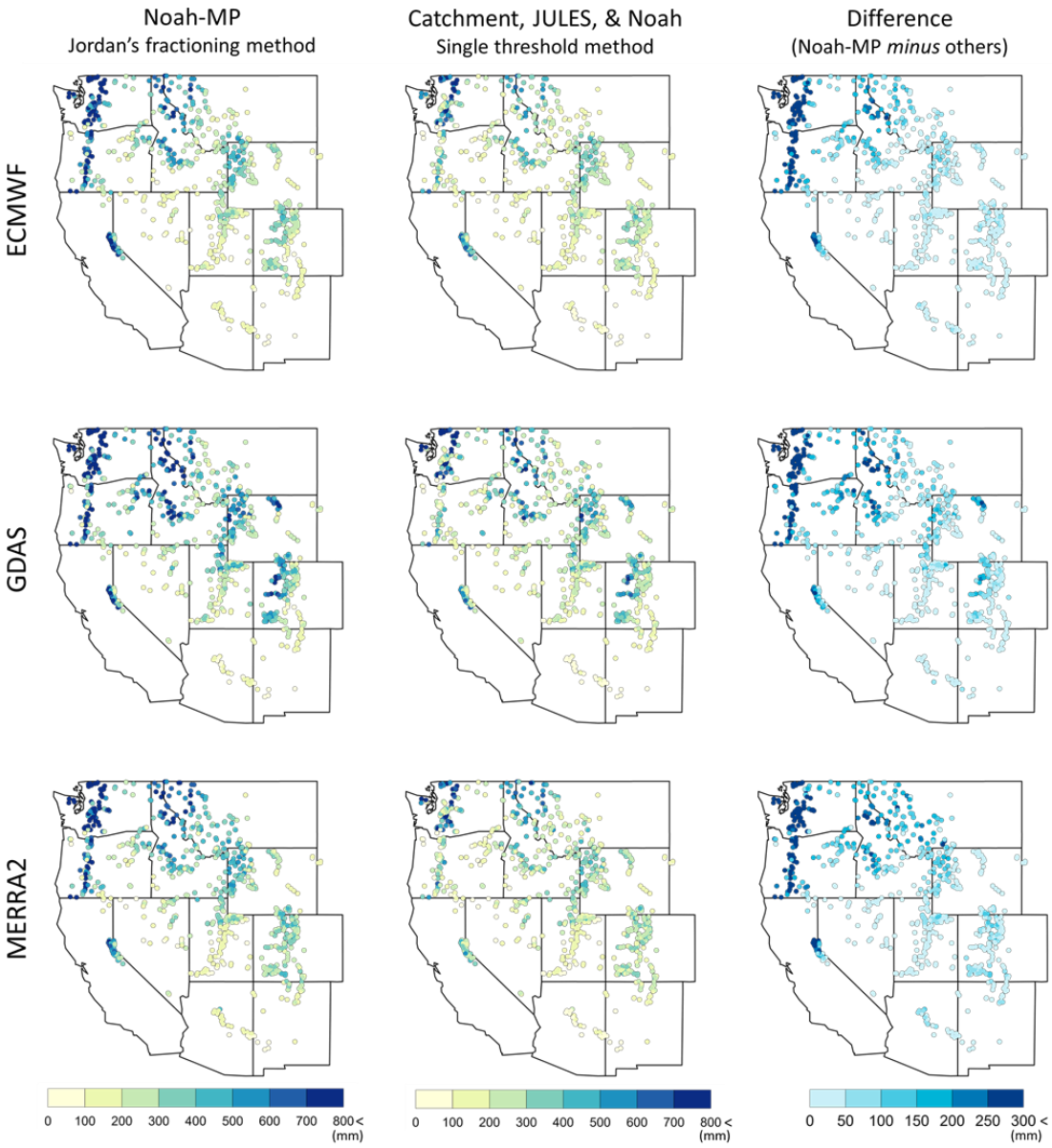

Figure S5. (a) Mean annual total snowfall maps from 2010 to 2017 during the accumulation period (Oct 1st to the date of the maximum SWE of each ensemble member) using Jordan (1991)'s fractioning method in Noah-MP and a single threshold method (0°C) in other three LSMs with the three meteorological forcings and their difference maps

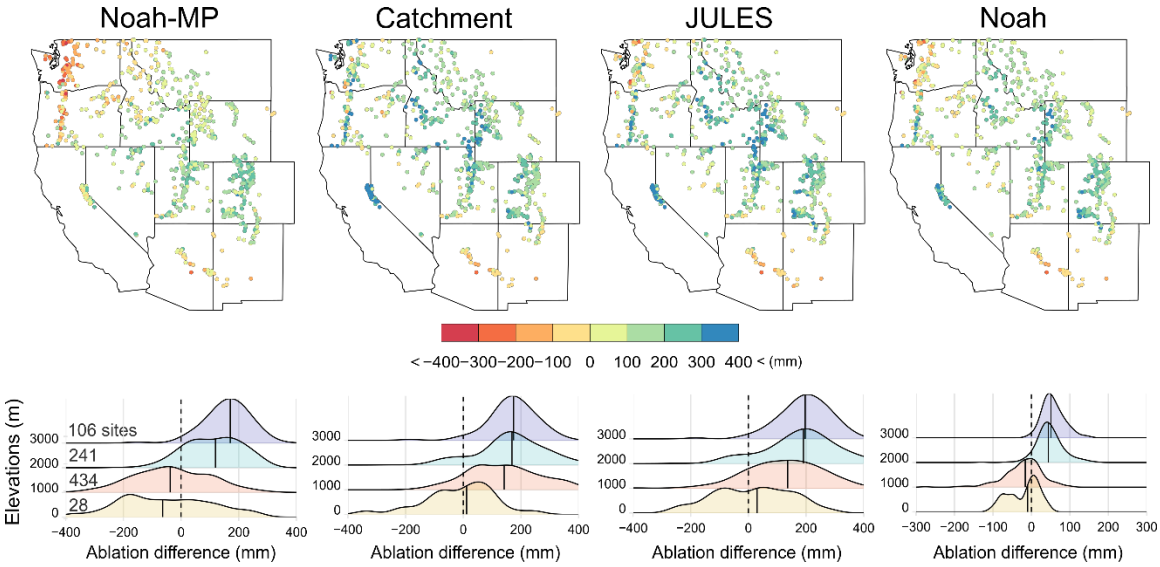

Figure S6. (a) Mean snow ablation difference maps (four LSMs ensembled by three forcings minus SNOTEL) during the accumulation periods from October 1 to April 1 for 2010 - 2017 across the western United States and (b) density plots of the snow ablation difference by four elevation ranges of SNOTEL sites

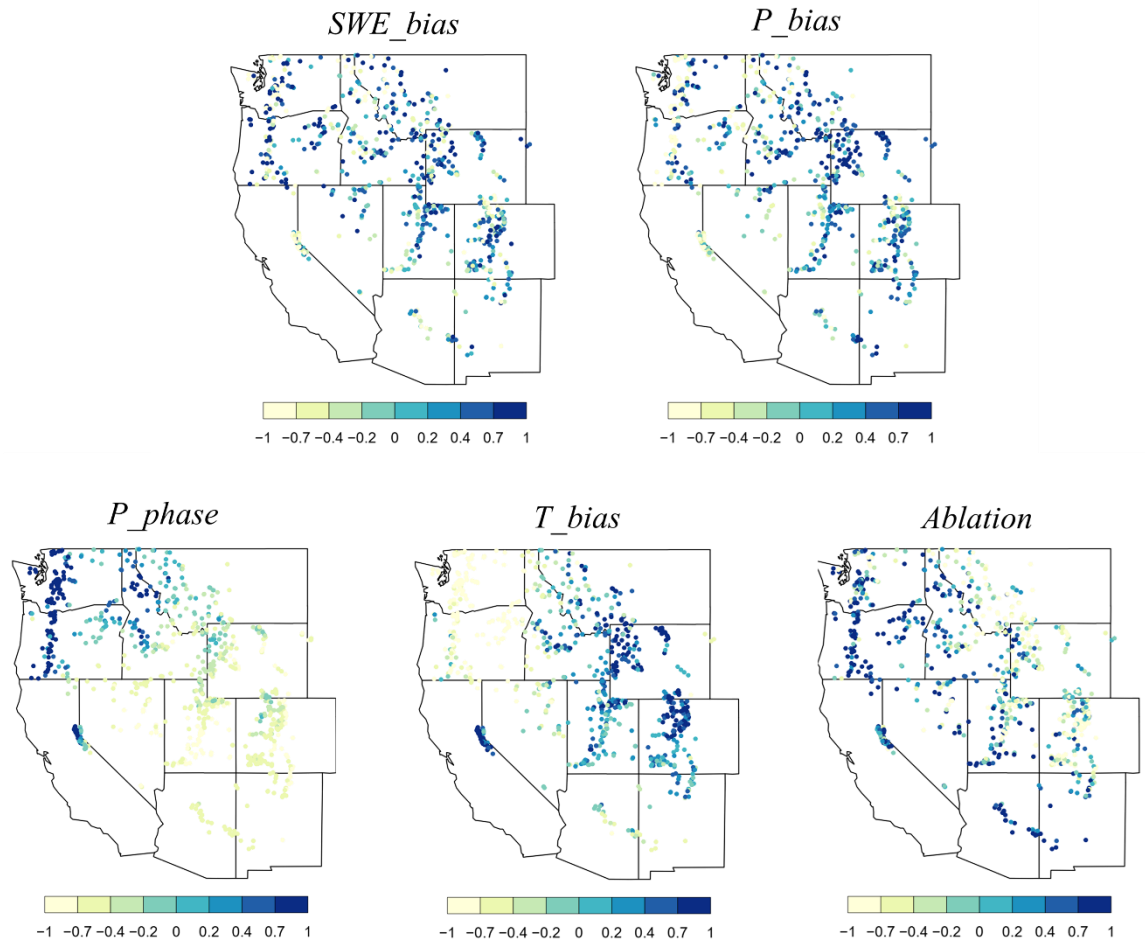

Figure S7. Standardized maps of SWE biases (*SWE_bias*) and four identified error sources (*P_bias*, *P_phase*, *T_bias*, and *Ablation*). Values of each variable were scaled such that the mean and standard deviation is zero and one, respectively.

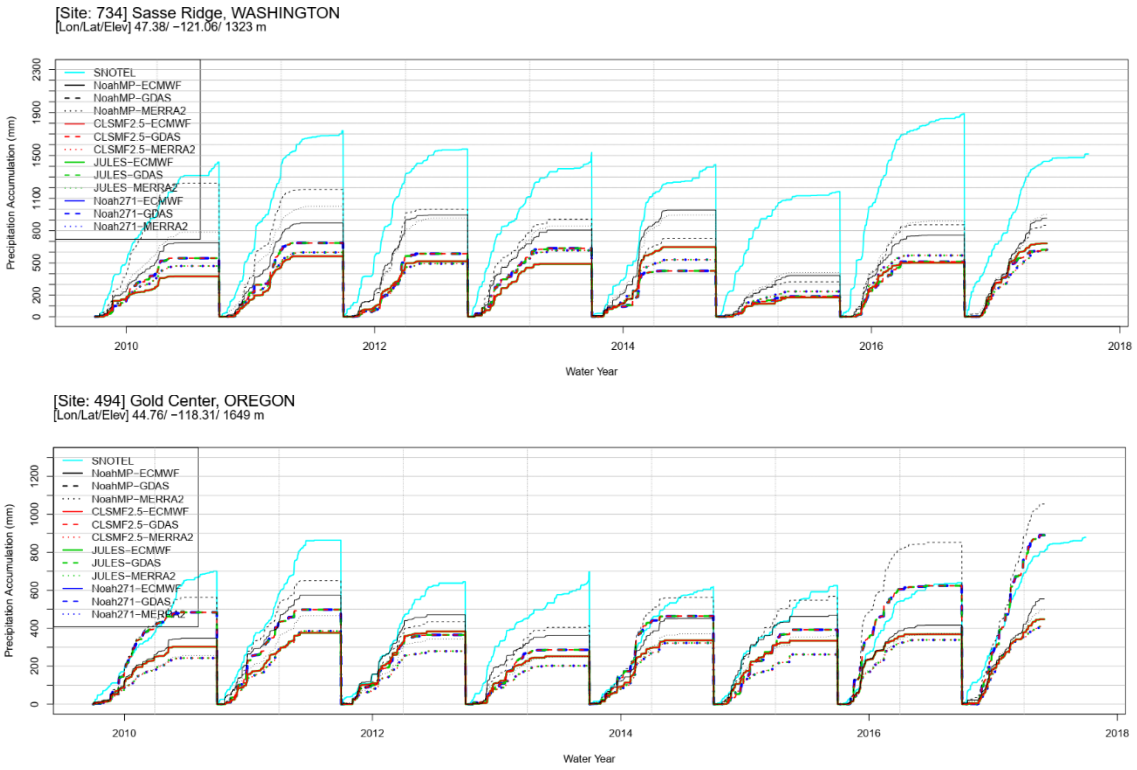

Figure S8. Time series of accumulated snowfall from three forcings (ECMWF, GDAS, and MERRA2) and accumulated total precipitation (snowfall + rainfall) from the SNOTEL data at two SNOTEL sites (Sasse Ridge, WA [No. 734] and Gold Center, OR [No. 494]) for eight water years from 2010 to 2017